

Dispersal of barnacle larvae along the central California coast: A modeling study

*Anna S. Pfeiffer-Herbert*¹

University of California, Santa Cruz, Ocean Sciences Department, 1156 High Street, Santa Cruz, California 95064

*Margaret A. McManus*²

Department of Oceanography, University of Hawaii at Manoa, Marine Sciences Building, 1000 Pope Road, Honolulu, Hawaii 96822

Peter T. Raimondi

University of California, Santa Cruz, Center for Ocean Health, Long Marine Lab, 100 Shaffer Road, Santa Cruz, California 95060

Yi Chao

Jet Propulsion Laboratory, California Institute of Technology, 4800 Oak Grove Drive, Pasadena, California 91109

Fei Chai

School of Marine Sciences, 453 Aubert Hall, University of Maine, Orono, Maine 04469

Abstract

To investigate the biological and physical mechanisms affecting larval dispersal, we embedded a model of *Balanus glandula* larval development and behavior into physical circulation fields of waters along the central California coast. Physical circulation fields were generated by a three-dimensional ocean circulation model with a horizontal resolution of 1.5 km and 20 topography-following layers in the vertical. The ocean circulation model was forced by air–sea fluxes derived from a mesoscale atmospheric model and assimilated temperature and salinity data from the Autonomous Ocean Sampling Network II experiment. An ecosystem model that calculated chlorophyll *a* (a proxy for larval food concentration) was also coupled to the ocean circulation model. The coupled model of larval development, larval behavior, food concentration, and physical circulation was used to run simulations of larval dispersal. Simulation results predicted a greater return of larvae to the nearshore waters with relaxation circulation patterns than with upwelling. More larvae were supplied to the coast north of Monterey Bay than to the south, and larvae that successfully returned to the nearshore waters generally had limited dispersal distances. These modeling results agree with previous observations of *B. glandula* population dynamics in central California.

Many intertidal marine species have a planktonic larval phase, and populations in the intertidal zone are largely shaped by the supply of these larvae. An understanding of the pathways of larval dispersal would provide many of the answers to questions about how intertidal populations are connected. However, direct observations of larvae dispersing in coastal waters are very sparse, because of the

difficulty of making these observations. An alternative to direct observation is to predict the paths of dispersing larvae with model simulations. In this study, we model the dispersal of *Balanus glandula* larvae and predict dispersal pathways in coastal waters of central California.

To model larval dispersal it is first necessary to understand the biology of the larvae. *B. glandula* is

¹ To whom correspondence should be addressed. Present address: Graduate School of Oceanography, University of Rhode Island, South Ferry Road, Narragansett, Rhode Island 02882 (annaph@gso.uri.edu).

² McManus previously Deksheniaks.

Acknowledgments

We thank Brian Grantham, Dave Lohse, Chris Edwards, Olivia Cheriton, and Shaun Johnston for helpful discussions regarding this manuscript. We are also grateful for the comments from two anonymous reviewers who made significant contributions to earlier versions of this manuscript. ROMS model output was prepared by Jei-Kook Choi. Francisco Chavez and Tim Pennington provided chlorophyll data from the Autonomous Ocean Sampling Network II experiment. *B. glandula* larval production and recruitment were measured by PISCO lab members Maya George, Hilary Hayford, and Carolina DaCosta; this data set was compiled by Dave Lohse.

Funding for this research was provided by the UC Marine Council for the Network for Environmental Observations of the Coastal Ocean (NEOCO) project, the Office of Naval Research grant N000140310267, and the Partnership for Interdisciplinary Studies of Coastal Oceans (PISCO), a long-term ecological consortium funded by the David and Lucille Packard Foundation. The research described in this paper was carried out in part at the Jet Propulsion Laboratory, California Institute of Technology, under contract with the National Aeronautics and Space Administration (NASA).

This is PISCO contribution 222.

a common barnacle found in the middle to upper rocky intertidal zone of the U. S. west coast (Strathmann 1987). The life history of *B. glandula* includes a planktonic larval phase and a sessile adult phase. There are six naupliar larval stages followed by a cyprid larva, which is specialized for settlement (Brown and Roughgarden 1985; Strathmann 1987). Larvae hatch in the mantle cavity of the adult and are released as stage I or II nauplii (Strathmann 1987). The naupliar stages are planktotrophic, and are thought to feed primarily on diatoms (Brown and Roughgarden 1985; Strathmann 1987). The duration of naupliar development in the field has been estimated as 2 to 4 weeks (Strathmann et al. 1981). The cyprid stage is nonfeeding, and the duration of this stage depends on stored lipid reserves, which typically support the cyprid larva for 3 to 4 weeks (Lucas et al. 1979), and the amount of time it takes the larva to reach suitable habitat. Larvae that successfully settle and metamorphose into a sessile juvenile are considered to be recruits to the intertidal population.

The second step in modeling larval dispersal is to quantify local circulation patterns in the region being studied. Three distinct circulation seasons have been identified along the central California coast: a spring and summer upwelling season, a fall transition, and a winter storm season (Breaker and Broenkow 1994). The movement of a high-pressure system in the North Pacific generates strong equatorward winds along the California coast during the spring and summer months. This wind stress causes offshore Ekman transport of surface waters along the coast, which is compensated for by upwelling of waters from depth (Breaker and Broenkow 1994; Rosenfeld et al. 1994). During the upwelling season there are periods of relaxation, when winds decrease in strength or reverse direction, resulting in an onshore movement of water, sometimes from as great as 200 m in depth. This alternate hydrographic state sets up and disappears rapidly with changes in the wind (Rosenfeld et al. 1994).

The coastal region that is considered in this study encompasses Monterey Bay, an open embayment measuring 37 km across its mouth (Breaker and Broenkow 1994) (Fig. 1). Upwelling strength in this region is observed to vary in intensity depending on local bathymetry. The amount of upwelling is particularly high in association with headlands (Rosenfeld et al. 1994). In the Monterey Bay region, upwelling activity is centered near Point Año Nuevo, which is located north of the bay, and Point Sur to the south (Breaker and Broenkow 1994; Rosenfeld et al. 1994). Plumes of upwelled water from these locations are advected southward, forming fronts between the cold upwelled water and warmer oceanic water (Rosenfeld et al. 1994). The Año Nuevo upwelling plume that crosses the mouth of Monterey Bay also establishes a second front between the upwelling plume and the surface water within the bay (Rosenfeld et al. 1994). As a dynamic response to upwelling, a cyclonic gyre forms in the interior of the bay (Graham and Largier 1997). This circulation feature acts to retain water inside the bay for approximately 8 to 12 d, which may help retain meroplankton locally (Graham and Largier 1997).

The final critical step in modeling larval dispersal is to describe how biological and physical factors interact to

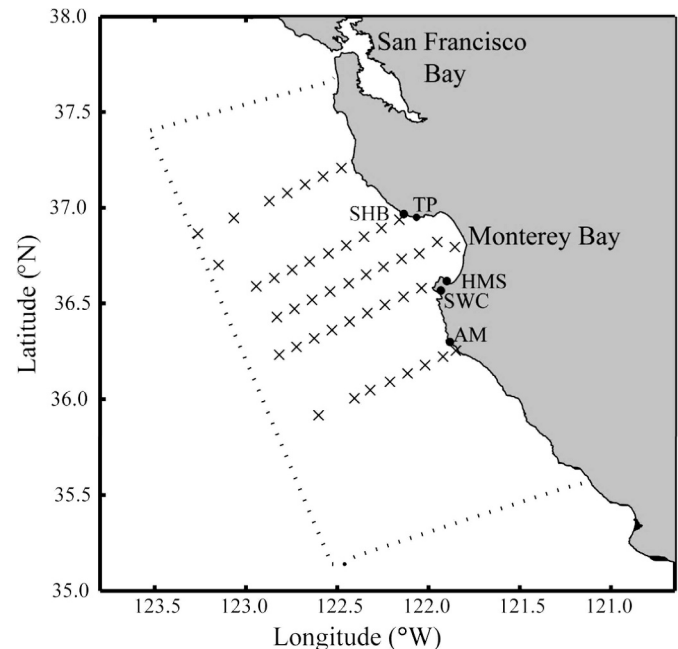


Fig. 1. Location of model domain on the central California coast. Domain boundary of 1.5-km horizontal resolution ROMS model configuration is indicated by the dotted line. Location of AOSN II profiles are shown by \times markers and PISCO sites are shown by filled circles labeled with site abbreviation (SHB, Sand Hill Bluff; TP, Terrace Point; HMS, Hopkins Marine Station; SWC, Stillwater Cove; AM, Andrew Molera State Park).

control the transport of larvae. While larvae are in the plankton, their horizontal movements are governed by physical circulation patterns, although the larvae are able to move in the vertical. Observational studies have shown a strong connection between upwelling/relaxation dynamics and barnacle recruitment along the central California coast. Roughgarden et al. (1991) present evidence that the offshore distance of *B. glandula* larvae is limited by an upwelling front, which is positioned further offshore under stronger upwelling conditions. These authors further hypothesize that larvae are able to settle in the intertidal zone when an upwelling front moves onto shore during a relaxation event (Roughgarden et al. 1991). Farrell et al. (1991) found that large pulses in recruitment to sites along the Monterey Peninsula on the southern end of Monterey Bay are correlated with wind relaxation, abrupt increases in temperature, and lowered salinity; all of these observations indicate that surface oceanic water had moved onshore and replaced the more dense upwelled water at the coastline during a relaxation event (Rosenfeld et al. 1994). A connection between wind patterns and settlement has also been observed for the larvae of crabs, sea urchins, and other species of barnacles (Wing et al. 1995; Bertness et al. 1996).

Measurements of barnacle larval recruitment along the west coast of the U.S. show variation over spatial scales of centimeters to hundreds of kilometers and timescales of days to years (Gaines et al. 1985; Connolly et al. 2001). The spatial variation in larval settlement that is observed in the intertidal zone is associated with spatially varying circulation patterns (Gaines et al. 1985; Botsford 2001). For

example, higher larval settlement is found near eddies that form next to the coast, in response to upwelling plumes, and retain larvae (Graham and Largier 1997; Botsford 2001). On a broader scale, a pattern of higher recruitment of *Balanus* spp. in the north compared with recruitment in the south has been widely observed along the U.S. west coast, and a similar pattern has been observed for both *Chthamalus* spp. and *Mytilus* spp. (Connolly et al. 2001). It is hypothesized that larvae are transported farther offshore in California because the strength of upwelling is greater than in Washington and Oregon, and thus it is more difficult for larvae to return to shore in California (Roughgarden et al. 1988; Connolly et al. 2001). Because the outcome of larval dispersal is highly influenced by ocean currents, it is important to consider how larvae interact with local, mesoscale, and regional circulation patterns.

Previous numerical models of *B. glandula* populations in central California point out the importance of connecting physical dynamics and larval dispersal (e.g., Roughgarden et al. 1988; Alexander and Roughgarden 1996). These studies provided important conclusions about the effects of large-scale circulation features on the supply of larvae to the near shore. The study presented in this paper extends this previous work by coupling an individual-based model of larval dispersal to realistic three-dimensional circulation, temperature, and chlorophyll fields modeled on a high-resolution grid. The coupled model is used to run simulations of larval dispersal within a domain that encompasses 350 km of coastline in central California and stretches approximately 150 km offshore (Fig. 1). Our simulations are designed to address a number of questions. First, do circulation patterns during relaxation events lead to increases in predicted larval supply to the near shore when compared with circulation patterns during upwelling events? Second, do larval dispersal dynamics vary along the central California coast? Finally, how does larval supply predicted by model simulations compare with observed patterns of larval recruitment?

Methods

Larval development model—The rate of *B. glandula* development through the naupliar larval stages is modeled as a function of temperature and food concentration (after Pfeiffer-Hoyt and McManus 2005). Temperature and food concentration parameterizations were based on previous laboratory studies that investigated the combined effects of temperature and food concentration on *B. glandula* naupliar development. In general, increases in temperature from 9°C to 16°C or food concentration from 0 to 50 $\mu\text{g L}^{-1}$ chlorophyll *a* (Chl *a*) (or both) increase the rate of larval development predicted by the model. The larval development model calculates the fraction of the total duration of the naupliar stages that is completed in the current time step.

Observations in the laboratory have shown that the duration of each naupliar stage is not an equal proportion of the total naupliar duration. To account for the observed difference in stage duration, each stage was assigned

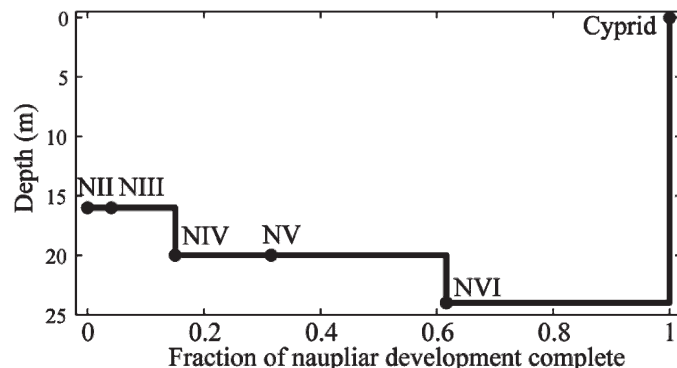


Fig. 2. Fraction of the total naupliar duration that is completed at the beginning of each naupliar stage versus stage-specific depth distributions of barnacle larvae. Larval stages are indicated by 'NII', 'NIII'... for 'Nauplius II', 'Nauplius III'..., respectively (data replotted, with permission, from Brown and Roughgarden, 1985). Mean (center of mass) depth of *Chthamalus* spp. larval stages collected in oblique net tows in the Monterey Bay region (B. A. Grantham, unpubl. data.).

a fraction of the total naupliar duration (Fig. 2). Stage I nauplii are nonfeeding and short-lived (<6 h), sometimes molting to stage NII before release, and are therefore not included in the larval transport simulations. For stages NII through NVI, the time for approximately half of the nauplii in one stage to molt to the next stage was divided by the average total naupliar duration in the Brown and Roughgarden (1985) experiment to obtain the relative fraction of time spent in each stage. Using these fractions, the amount of time needed to complete each stage is back-calculated from the total naupliar duration. A detailed description of the larval development model is given in Pfeiffer-Hoyt and McManus (2005).

Larval depth distributions—Laboratory studies have shown that the phototaxis and pressure response behavior of barnacle larvae changes through the naupliar and cyprid stages (Knight-Jones and Morgan 1966; Lang et al. 1979); thus, it is likely that the depth distributions also change. Direct observations of the depth distributions of barnacle larvae in the Monterey Bay region have been made for *Chthamalus* spp. larvae that were collected in depth-stratified plankton tows along six cross-shore transects taken in 1993–1994 (B. A. Grantham pers. comm.). The center of mass by depth of the NII–III, NIV–V, and NVI *Chthamalus* spp. larval stages was found to increase with larval maturity (Grantham pers. comm.) (Fig. 2). An increase in average depth with naupliar stage has also been observed for *Balanus improvisus* (Bousfield 1955) and other central California barnacle species (Grantham pers. comm.). Because *B. glandula* larvae have not been sampled at discrete depths over long periods of time or spatial extents, the detailed *Chthamalus* spp. observations are used in model simulations to represent the average depth that a distribution of larvae occupies during each naupliar stage. The model results were not very sensitive to the assumed depth distribution (see 'Model sensitivity'). *B. glandula* cyprids have been frequently observed at the surface in the

nearshore waters (Grosberg 1982), and are observed to settle exclusively near the surface on moorings in greater than 60 m depth in Monterey Bay; therefore the cyprid stage is transported at the surface in model simulations. In the simulations of larval transport, it is assumed that larvae are able to maintain their preferred depth, and that they are not perturbed significantly by vertical velocities. Measured swimming speeds of barnacle nauplii range from 0.4–1.1 cm s⁻¹ (Hardy and Bainbridge 1954; Wu et al. 1997) and for cyprids range from 0.2–0.5 cm s⁻¹ (De Wolf 1973). In comparison, vertical current speeds measured at fronts are no more than 0.02 cm s⁻¹ (Franks 1992). Additionally, observations of zooplankton distributions in relation to turbulent flow caused by a storm in Monterey Bay suggested that the stronger swimming copepods, which have observed swimming speeds of ~0.4 cm s⁻¹ (Yamazaki and Squires 1996), were able to regulate their depth despite the strong mixing conditions (Haury et al. 1990). Thus, it is highly likely that barnacle larvae are capable of overcoming most of the vertical velocities that they will experience.

Fields of velocity, temperature, and chlorophyll—Horizontal current velocities generated by the Regional Ocean Modeling System (ROMS) were used to calculate the trajectories of larvae within the Monterey Bay region. ROMS solves the primitive equations in an Earth-centered rotated Cartesian system of coordinates. ROMS is discretized in coastline- and terrain-following curvilinear coordinates. ROMS is a split-explicit, free-surface ocean model, where short time steps are used to advance the surface elevation and barotropic momentum, with a much larger time step used for temperature, salinity, and baroclinic momentum. For the Monterey Bay region, ROMS configurations are nested at three levels: the U.S. West coastal ocean at 15 km resolution, the central California coastal ocean at 5 km resolution, and Monterey Bay at 1.5 km resolution. The 1.5-km ROMS domain is shown in Fig. 1. All three ROMS configurations have 20 vertical sigma layers. The 15-km, 5-km, and 1.5-km regional ROMS are nested on-line as a single system and run simultaneously exchanging boundary conditions one way at every time step of the parent grid.

The ROMS configuration described above has been integrated for many seasonal cycles starting from the climatological conditions and forced by the climatological air–sea fluxes. During the August 2003 integration, the air–sea fluxes were derived from the Coupled Ocean–Atmosphere Mesoscale Prediction System (Hodur 1997) at 3-km resolution. Ocean temperature and salinity measurements collected from both remote sensing (e.g., satellites and aircraft) and in situ platforms (e.g., ships, gliders, autonomous underwater vehicles) during the Autonomous Ocean Sampling Network II (AOSN II) project of August 2003 were assimilated into ROMS using a three-dimensional variational method. Snapshots of the model output saved daily were used in the coupled model presented here.

ROMS is developed with an aim to be a multipurpose, multidisciplinary oceanic modeling tool. The modularity of the ROMS code also allows us to configure and explore

alternative ecosystem model formulations. During the AOSN II project, an ecosystem model (Carbon, Silicate, and Nitrogen Ecosystem—CoSINE), developed by Chai et al. (2002), was embedded into the three-level nested ROMS. The CoSINE consists of 10 compartments: two classes each of phytoplankton (P1, P2) and zooplankton (Z1, Z2), dissolved inorganic nitrogen in the form of nitrate (NO₃) and ammonium (NH₄), detritus nitrogen, silicate (Si(OH)₄), detritus silicate (DSi), and total CO₂ (TCO₂) (Fig. 3). Nitrate and ammonium are treated as separate nutrients, thus dividing primary production into new production and regenerated production. Sinking particulate organic matter is transformed into inorganic nutrients by a two-step regeneration process first to NH₄, then to NO₃. The sinking flux of particulate matter is specified using an empirical function similar to the one used by Chai et al. (1996). The regeneration of silicate is modeled by incorporating the DSi dissolution rate, which varies with the water temperature (Jiang et al. 2003).

All the biogeochemical fields (e.g., nutrients, plankton, and TCO₂) were initialized from the Pacific ROMS-CoSINE model simulation (50-km resolution) with climatological July values. Boundary conditions for the biogeochemical components were also used from the Pacific ROMS-CoSINE outputs. The three-level nested ROMS-CoSINE model has been simulated for the period of the AOSN II, August 2003, during which the high-resolution (3-km) surface daily wind is available to force the model. The coupled ROMS-CoSINE model captures many observed features during the AOSN II period.

We performed a detailed comparison of modeled chlorophyll with in situ observations. The modeled chlorophyll concentration is derived from the phytoplankton biomass concentration (mmol N m⁻³), converted to mg m⁻³ using a nominal gram chlorophyll-to-molar nitrogen ratio of 1.64, corresponding to a chlorophyll-to-carbon mass ratio of 1 : 50 and a C : N molar ratio of 7.3.

We compared 124 chlorophyll profiles measured from shipboard 02–06 August and 21–25 August 2003 during the AOSN II experiment, with chlorophyll predicted by ROMS-CoSINE at the same locations. Overall, the model predicted chlorophyll very well. Chlorophyll predicted by the model ranged from 0 to 24 µg L⁻¹ Chl *a*, whereas the measured chlorophyll ranged from 0 to 30 µg L⁻¹ Chl *a*. The root mean square (RMS) difference for each profile ranged from 0.5 to 2.3 µg L⁻¹ Chl *a*, with a mean of 0.7 µg L⁻¹ Chl *a*. From 0- to 30-m depth the measured chlorophyll was slightly higher than the chlorophyll predicted by the model; this effect was pronounced at the chlorophyll maximum. In 75% of the profiles, the measured peak chlorophyll abundance was greater than the predicted peak. To account for the possible underprediction of chlorophyll concentration by the model, the ROMS-CoSINE chlorophyll fields were augmented by the mean difference of 0.7 µg L⁻¹ Chl *a*.

Calculation of larval trajectories—The boundary of ROMS circulation model occurs roughly 2 km from the shoreline. Stage II nauplii are spawned into the model at this ROMS boundary. The assumption is made that feeding

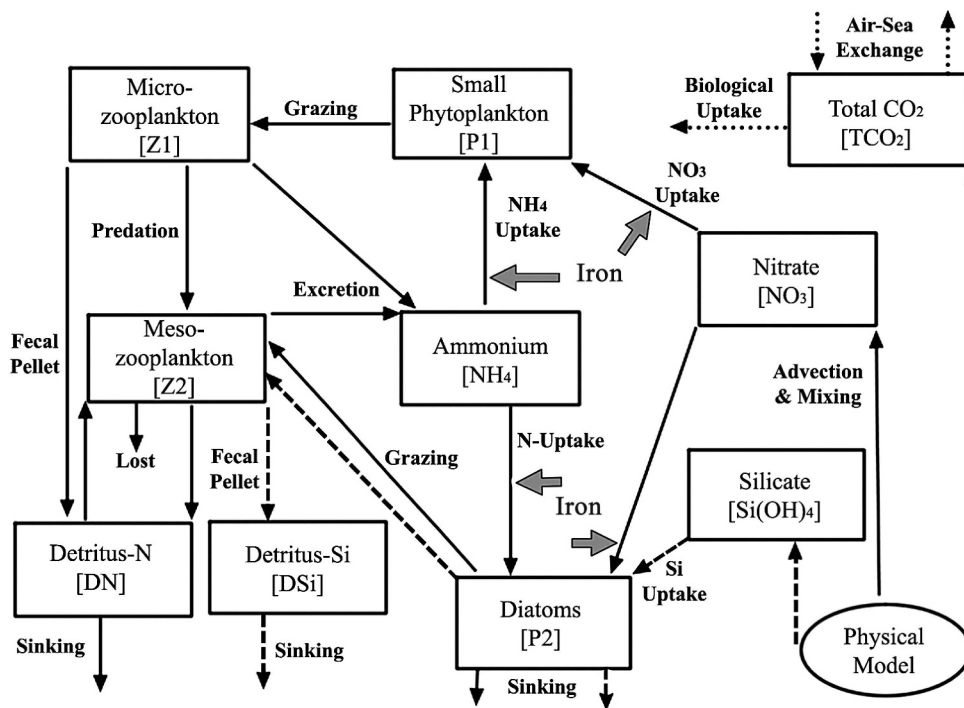


Fig. 3. Schematic of ROMS-CoSINE physical-ecosystem model structure (from Chai et al. 2002). P1 represents small, easily grazed phytoplankton whose specific growth varies, but whose biomass is regulated by micrograzers (Z1) and whose daily net productivity is largely remineralized. P2 represents relatively large phytoplankton ($>10 \mu\text{m}$) that makes up high biomass blooms and contributes disproportionately to sinking flux as ungrazed production or large fecal pellets. The P2 class represents the diatom functional group, and has the potential to grow fast under optimal nutrient conditions, such as iron. Z1 represents small micrograzers whose specific growth rates are similar to P1 phytoplankton and whose grazing rates are density dependent, and Z2, the larger mesozooplankton that graze on P2 and detrital nitrogen (DN) and prey on Z1. Solid arrows show the path of N, dashed arrows show the path of Si, and dotted arrows show the path of CO_2 . At the points indicated by gray arrows the uptake rates are a function of iron availability.

nauplii, released on the shoreline, are instantaneously translocated to the ROMS model boundary. Using the transport rates calculated from in situ Acoustic Doppler Current Profiler (ADCP) data from the Partnership for Interdisciplinary Studies of Coastal Oceans (PISCO) at two representative sites in the model domain, stage II nauplii would reach the ROMS boundary within 1.2 d at the Terrace Point (TP) site and within 2.5 d at the Stillwater Cove (SWC) site (Fig. 1). This is a small fraction of the development time for the larvae that does not significantly affect the overall dispersal distances of these larvae.

Simulated larvae are tracked as particles within horizontal current velocity fields. The trajectory of an individual larva is calculated numerically by fourth-order Runge-Kutta integration. Naupliar development rate is calculated once per day (as a function of temperature and chlorophyll), and larval movement is calculated every 30 min. At each 30-min time step, a new latitude and longitude position of each larva is calculated from the current velocity vectors, and temperature and chlorophyll concentrations are recorded at the new position. Larvae that cross the seaward boundaries of the domain are considered lost from the simulation. Larvae that cross the

shore boundary are returned inside the boundary and held there unless a change in current velocity carries the larva away from the shore. At the end of a full day, the stored temperature and chlorophyll values output from the ROMS model are averaged, and the average values are used to calculate the fraction of development that was completed during that day using the naupliar development model. The vertical position of the larva is determined by the amount of maturation (i.e., life stage) that the larva has completed. When a larva reaches the cyprid stage, the position of the cyprid continues to be tracked until the cyprid is either lost through the sea boundaries of the domain or arrives within 2 km of shore (the inshore boundary of the ROMS model), where it is counted as a settler. The duration of the cyprid stage was not given an upper limit aside from the total simulation duration of 45 d. At the end of a simulation, larvae that arrived within 2 km of the coastline at any time during the simulation after maturing to the cyprid stage are considered settled larvae. It is important to note that the model predicts potential settlement, as opposed to actual settlement, because it does not include processes in the very nearshore waters that can influence settlement, such as larval settling

Table 1. Summary of simulation conditions.

Simulation	Hydrographic state	Temperature	Chlorophyll	Duration
1	Upwelling	Uniform	Uniform	45 d
2	Relaxation	Uniform	Uniform	45 d
3	Upwelling & Relaxation	Variable	Variable	45 d
4	Upwelling & Relaxation	Variable	Variable	45 d

behavior (Raimondi 1988), predation (Gaines and Roughgarden 1987), or the suitability of the local habitat (Berntsson et al. 2004).

Simulations—Simulations of larval dispersal were run using the interpolated fields of current velocity, temperature, and chlorophyll (Table 1). In simulations 1–3, larvae were released from 700 starting positions along the coastline, located 1 km apart, at the average naupliar stage II depth (Fig. 2). In simulations 1 and 2, temperature and chlorophyll were assigned uniform values to investigate the effects of variations in upwelling and relaxation circulation patterns alone. A temperature of 14.5°C and chlorophyll of 5 $\mu\text{g L}^{-1}$ Chl *a* were selected as average after a close examination of temperature and chlorophyll measurements collected shipboard during the AOSN II experiments. This combination leads to a calculated naupliar duration of 21 d. With this naupliar duration, the total simulation duration of 45 d allows cyprid durations of up to 24 d, which is within the range of potential cyprid duration determined by calculations of energetics and laboratory experiments (Lucas et al. 1979; Strathmann et al. 1981). Simulation 1 was run with constant upwelling conditions using velocity fields from 12 August 2003, and simulation 2 was run with constant relaxation conditions using velocity fields from 21 August 2003 (Table 1). The day of 12 August 2003 was chosen to represent conditions of upwelling and 21 August 2003 was chosen to represent conditions of relaxation. These days were chosen by surface wind direction at National Data Buoy Center (NDBC) buoy 46042, located at 36°75'N, 122°42'W (http://www.ndbc.noaa.gov/station_history.php?station=46042, Fig. 4), patterns of sea surface temperature from ROMS output data,

and personal observations of the authors aboard the *RV Pt. Sur* during the AOSN II experiments.

Simulation 3 was run with daily-varying hydrographic conditions, temperature, and chlorophyll fields typical of the days between 01 August and 31 August 2003 (Table 1). The simulation began on 01 August 2003 and ran for a total duration of 45 d by looping back to the beginning of the month. Simulation 4 had the same conditions as simulation 3, but larvae were released in clusters adjacent to five intertidal sites that are monitored by PISCO (Fig. 1). In simulation 4, 80 larvae were released from each PISCO site.

Results

Simulations 1–3 were run with larvae released from 700 positions that were evenly spaced (1 km) along the coastline. In simulation 1, larval transport was simulated under constant upwelling conditions and with uniform temperature and chlorophyll. The larval trajectories calculated in this simulation were generally offshore and southward, and many of the trajectories exited the southern boundary of the model domain (Fig. 5A). In total, 11% of the larvae reached within 2 km of the shoreline after maturing to the cyprid stage, and thus were counted as settled larvae (Table 2). In simulation 2, larval transport was simulated with constant relaxation conditions and uniform temperature and chlorophyll. In this simulation, many of the larvae traveled onshore or northward (Fig. 5B). In comparison with the simulation with constant upwelling (simulation 1), fewer larvae exited the model domain. By the end of simulation 2, 76% of the larvae settled (Table 2). There is a clear difference in the settlement success of larvae in simulation 1 and simulation

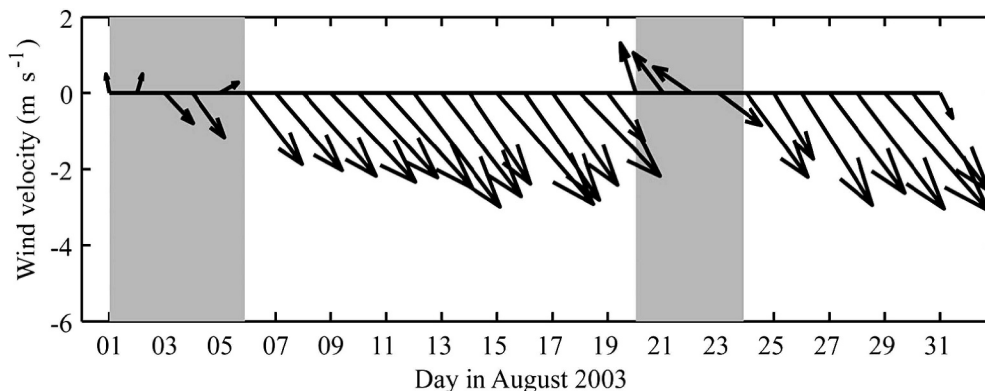


Fig. 4. Time series of wind velocity. Wind vectors from NDBC buoy 46042 averaged by day from 01 to 31 August 2003. Shaded areas indicate periods of relaxation from upwelling conditions.

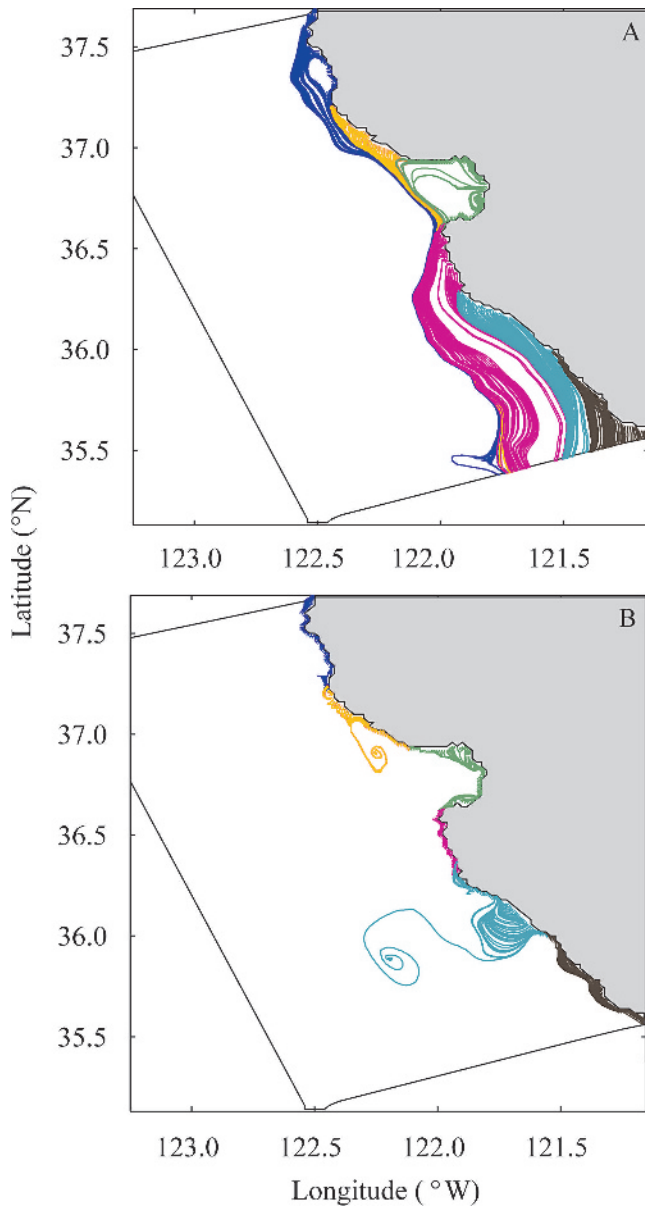


Fig. 5. Larval dispersal paths calculated with (A) constant upwelling (simulation 1) and (B) constant relaxation (simulation 2). Dispersal paths are colored by the release location: from the northern boundary to Point Año Nuevo (dark blue), Point Año Nuevo to Monterey Bay (gold), Monterey Bay interior (green), Monterey Bay to Point Sur (magenta), south of Point Sur (light blue), and southernmost shoreline (brown).

2, with much higher settlement occurring under relaxation conditions. This result suggests that relaxation circulation patterns promote larval settlement, which is supported by previous observations of barnacle larval settlement in Monterey Bay (Farrell et al. 1991; Roughgarden et al. 1991).

In simulation 3, circulation patterns, temperature, and chlorophyll all varied daily. By the end of simulation 3, 5% of the larvae settled within the model domain (Table 2). A majority (76%) of the successful larvae settled either north of Monterey Bay or within the northern half of the bay. Successful settlers traveled from 4 to 128 km along the coastline, with a median dispersal distance of 23 km. Only 12% of the settlers traveled farther than 50 km. Of these, all but one were released just south of Point Año Nuevo, at the origin of a plume of upwelled water that often crosses the mouth of Monterey Bay during upwelling conditions (Rosenfeld et al. 1994). Three patterns emerge from the dispersal paths calculated in simulation 3. First, in comparison with simulations with static circulation patterns, larvae dispersed to more areas of the domain. In particular, many larvae were carried out to sea through the western boundary during simulation 3, whereas most larvae stayed within 25 km of the shoreline in simulations 1 and 2 (constant circulation). Second, there appears to be a barrier to dispersal at Point Sur, a headland 35 km south of Monterey Bay. Very few larvae released north of Point Sur approached the coastline to the south, and likewise, very few of the larvae approached the northern coastline when released south of Point Sur (Fig. 6). Third, larval dispersal paths approached the outer Monterey Peninsula, on the southern mouth of Monterey Bay, from many parts of the coast north of the bay. This peninsula appears to be the major landfall for larvae that are transported by the Año Nuevo upwelling plume.

In simulation 4, larvae were released from five sites monitored by PISCO. Overall, 5% of these larvae settled within the model domain. The success of larvae released from each PISCO site was measured by the number of larvae that settled along the coastline anywhere within the model domain. Sand Hill Bluff (SHB) and TP had the greatest number of successful larvae (8% and 11%, respectively). SWC had fewer successful larvae (4%), and none of the larvae released from Hopkins Marine Station (HMS) or Andrew Molera State Park (AM) successfully settled within the model domain. Overall, dispersal distances of successful larvae in simulation 4 ranged from 9 to 29 km, with a median distance of 18 km. Of the release sites with successful larvae, the median dispersal distance

Table 2. Summary of simulation results: simulations 1–4.

Simulation	Settled (%)	Dispersal distance* range (km)	Mean dispersal distance (km)	Median dispersal distance (km)
1	10.9	0.1–8.5	3.5	2.9
2	75.9	0.5–55	8.7	2.9
3	4.9	3.6–128	27	23
4	4.5	9.4–29	18	18

* Distance along the coastline between starting and ending position of settled larvae.

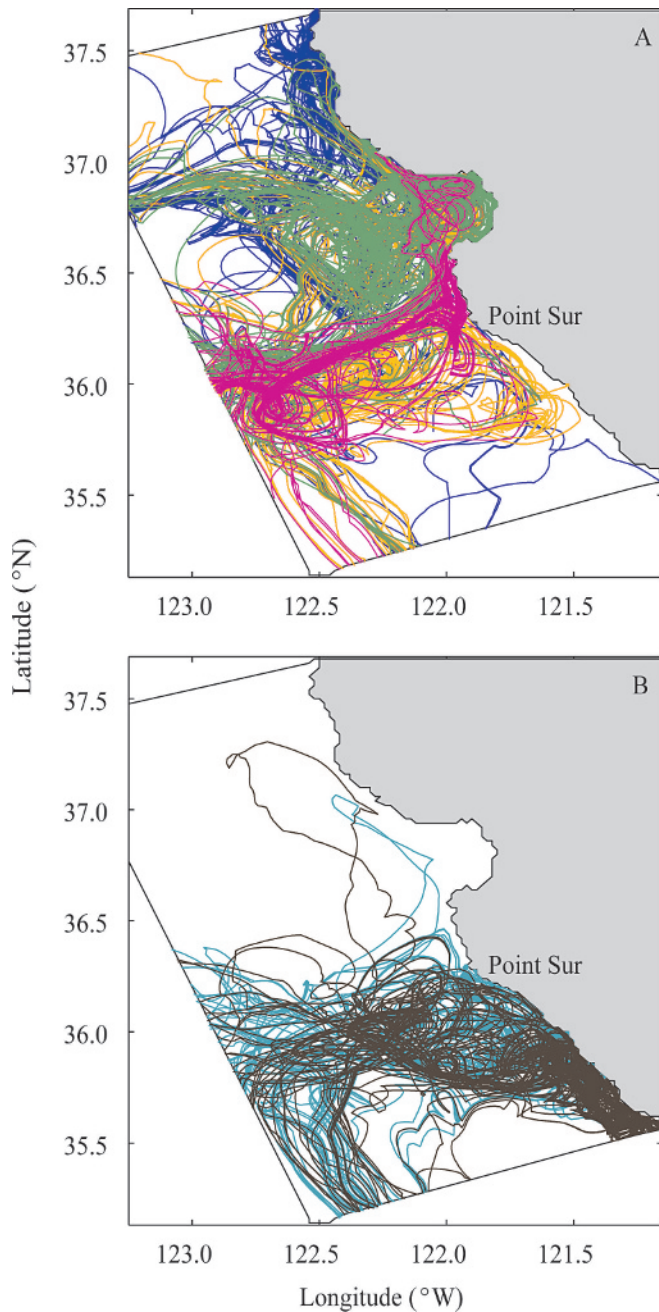


Fig. 6. Larval dispersal paths calculated in simulation 3. (A) Larvae released north of Point Sur. (B) Larvae released south of Point Sur. Dispersal paths are colored by the release location: from the northern boundary to Point Año Nuevo (dark blue), Point Año Nuevo to Monterey Bay (gold), Monterey Bay interior (green), Monterey Bay to Point Sur (magenta), south of Point Sur (light blue), and southernmost shoreline (brown).

was greatest from SHB (21 km) and least from SWC (10 km).

The dispersal paths of larvae released in simulation 4 show that larvae that successfully settled traveled close to the coast inside Monterey Bay and north of the bay. In contrast, dispersal paths of unsuccessful larvae diverge away from the coast south of the Monterey Peninsula

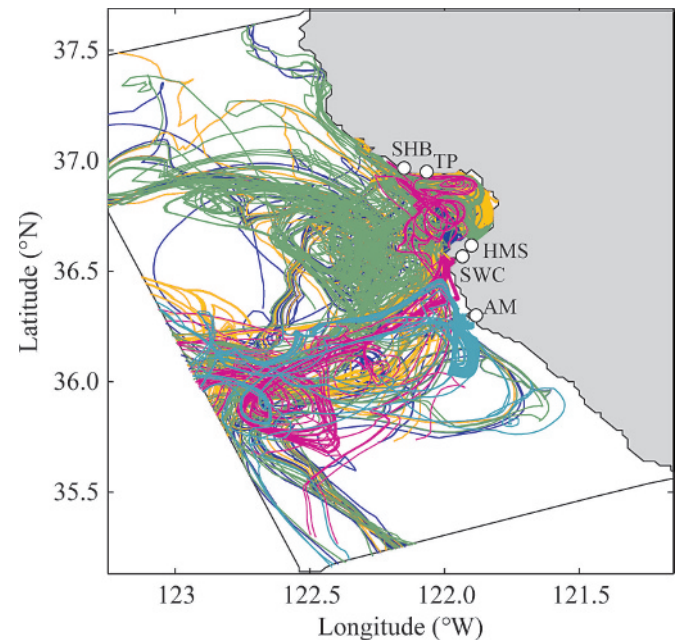


Fig. 7. Larval dispersal paths calculated in simulation 4. PISCO intertidal sites are indicated by white circles along the coastline. Dispersal paths are colored by release site: Sand Hill Bluff (SHB, dark blue), Terrace Point (TP, gold), Hopkins Marine Station (HMS, green), Stillwater Cove (SWC, magenta), and Andrew Molera State Park (AM, light blue).

(Fig. 7). Many of the larvae released from SHB and TP circulated in the counterclockwise eddy that is typical in Monterey Bay during upwelling conditions and then either headed north close to the coastline or out of the domain to the west. Dispersal paths from SHB approached Monterey Peninsula, while dispersal paths from TP stayed further in the interior of Monterey Bay. Most of the larvae released near HMS initially traveled onshore and remained there until carried up into the bay by changing currents. In the natural environment, some of these larvae would probably be retained by fine-scale nearshore circulation features until they could mature and settle. High retention of larvae near HMS is supported by a strong correlation between larval production at HMS and subsequent recruitment (D. Lohse pers. comm.). Some of the larvae released near SWC were retained within this cove for a short time before traveling north into Monterey Bay. All other dispersal paths from this site trended offshore. Nearly all of the dispersal paths from AM, which is located on Point Sur, trended out to sea and did not approach the coastline to the north or south of the point.

Model sensitivity—The sensitivity of model results to three parameterizations (larval depth distribution, magnitude of temperature and chlorophyll, and initial position) was examined through a series of simulations. First, the sensitivity of model predictions to the observed depth distribution was tested by running simulation 3 with an alternate distribution of larval depths. In the alternate depth distribution simulation, naupliar depth increases by 5 m with each stage, from stage NII at 5 m to stage NVI at

Table 3. Results of sensitivity analyses with simulation 3.

Change to simulation	Difference in settlement* (%)
Depth distribution	-3.5
Temperature increased	-3.5
Temperature decreased	-4.6
Chlorophyll increased	5.1
Chlorophyll decreased	-4.9
Starting positions	-4.6
Simulation 1†	6.0
Simulation 2	71.0

* Difference calculated by subtracting percentage settled in simulation 3 from percentage settled in the altered simulation.

† Simulations 1 and 2 are included as a comparison with sensitivity analysis results.

25 m, and cyprids returned to the surface. Second, we tested the model's sensitivity to perturbations in the temperature and chlorophyll fields. In four separate simulations, the temperature fields were uniformly shifted by $\pm 1^\circ\text{C}$ and the chlorophyll fields by $\pm 0.7 \mu\text{g L}^{-1}$ Chl *a*. These values were chosen because the ROMS model predictions of temperature had RMS error of as much as 1°C in comparison with in situ profiles. In addition, in comparison with 124 profiles of chlorophyll measured by fluorometer, the coupled ROMS ecosystem model had a RMS error of 0.5 to $2.3 \mu\text{g L}^{-1}$ Chl *a*, with a mean and median of $0.7 \mu\text{g L}^{-1}$ Chl *a*. Finally, we tested the sensitivity of the model output to the initial positions of larvae; the initial starting positions used in simulation 3 were moved by 0.0025° to the south and to the west.

Results from the sensitivity analysis simulations in comparison with simulation 3 are given in Table 3. Changes in chlorophyll concentration led to the greatest difference in settlement ($\pm 5\%$), while changing the depth distribution of the larvae or increasing temperature resulted in the smallest difference in settlement (-3.5%). These differences are small compared with differences in settlement between simulations with constant upwelling (simulation 1) and constant relaxation (simulation 2) as compared with simulation 3 (Table 3). These sensitivity analysis simulations give us a window of results for simulation 3. Predicted settlement ranges from 0% to 10%, and dispersal distances range from 1 to 360 km with a mean of 30 km. Another consistent result is that more larvae settled in the northern half of the domain than the southern half in every simulation except increased temperature.

Discussion

In larval transport simulations with uniform temperature and chlorophyll, more larvae returned to the coastline with relaxation circulation patterns (simulation 2) than with upwelling circulation (simulation 1). This result agrees with previous observations of associated pulses of barnacle recruitment in Monterey Bay with relaxation events (Farrell et al. 1991; Roughgarden et al. 1991). The settlement locations from simulations 1 and 2 also suggest that settlement on the open coastline may rely on relaxation

events more than settlement within Monterey Bay, where larvae can be retained by a recirculation during upwelling. Settlement predicted by the upwelling simulation is strongly concentrated in Monterey Bay, whereas settlement predicted by the relaxation simulation is more evenly distributed along the coastline. With temporal variation of upwelling and relaxation conditions and spatial variation in temperature and chlorophyll (simulation 3), the number of settled larvae was less than the two simulations with constant circulation (simulations 1 and 2). The distance that successful larvae dispersed from their release point was no more than 128 km and the median dispersal distance was approximately 23 km. In contrast, given that alongshore currents of $10\text{--}20 \text{ cm s}^{-1}$ are observed on the continental shelf of central California (Rosenfeld et al. 1994) and the predicted duration of the naupliar period is 15–25 d in Santa Cruz, California (Pfeiffer-Hoyt and McManus 2005), potential dispersal distances of *B. glandula* larvae are at least 150–500 km. The shorter dispersal distances predicted by model simulations is supported by a study of population genetics, which found that average dispersal distances must be limited in central California (Sotka et al. 2004). Our simulation results support the proposal that the exchange of larvae is restricted by circulation patterns in central California (Connolly et al. 2001; Sotka et al. 2004).

One goal of modeling larval dispersal is to help explain patterns observed in intertidal populations. Larval recruitment data have been collected at the five PISCO sites for the past 5 yr. To assess how well the model simulations replicated observations, we compared predicted larval supply to PISCO observations of barnacle recruitment. In PISCO observations, there is a more than 10-fold difference between recruitment in sites to the north of Monterey Bay and sites to the south, which agrees with the general trend of barnacle recruitment increasing with latitude (Connolly et al. 2001). Potential settlement predicted by simulation 3 closely follows this observation, with 76% of the successful larvae settling north of the middle of Monterey Bay. Differences between the predicted supply of larvae and observed recruitment may be attributable to settlement and postsettlement processes. In addition to potential settlers, the model simulations predict paths of larval dispersal for August 2003. Very few of these dispersal paths approached the coast near the PISCO observation sites. Compared with the 2003 average, observed larval recruitment was low in August and September 2003. The dispersal paths predicted by the model suggest that the observed low recruitment at PISCO sites during the late summer may be related to low larval supply.

Model limitations and applications—Modeling larvae as particles with growth and behavior in three-dimensional circulation fields is one method of tracking the dispersal pathways of larvae. Through this type of modeling, environmental parameters can be prescribed, the location of each individual larva is known over time, and predictions can be made through repeated model simulations. However, modeling is a just one tool that can be used to reveal the linkages between the adult spawning population

and the recruits, and this tool has inherent uncertainties. Model predictions are limited by our knowledge of the important biological processes involved in larval dispersal. The model simulations presented in this paper include two key biological assumptions. First, larval development rate is predicted from relations that were discovered in the laboratory. The model assumes that these relations apply to the natural environment as well (Pfeiffer-Hoyt and McManus 2005). Second, larval behavior is derived from a different species of barnacle. Although there are indications that *B. glandula* larvae exhibit similar swimming behavior in the field, there have been no extensive observational studies. Thus, to improve our model predictions, both larval development and behavior need to be better characterized by observation in the field.

Although coupled ecosystem models such as ROMS-CoSINE have become very accurate at predicting phytoplankton abundance on the scale of kilometers, these models are unable to resolve finer-scale patchiness of chlorophyll that is observed in the field. For example, phytoplankton can be three to five times more abundant in thin layers of a few centimeters to a few meters in depth compared with the abundances above or below the thin layer (McManus et al. 2003). Again, to improve our predictions of the natural environment, these finer-scale variations in chlorophyll need to be accounted for.

Our model predicts the potential supply of larvae to the nearshore waters, while observations of larval recruitment are taken after settlement and postsettlement processes have taken place. Filling the gap between supply to the nearshore region and recruitment will require three components. First, the physical circulation fields obtained from ROMS do not include very nearshore currents. Nearshore circulation patterns will need to be understood in greater detail before we can predict the delivery of larvae directly into the intertidal zone. Second, studies have shown that the settlement of larvae once they reach the intertidal zone is determined by larval behavior (e.g., Berntsson et al. 2004). Understanding how barnacle larvae choose a location to settle will improve our ability to predict where settlement will occur after the larvae are delivered near their habitat. Third, postsettlement survival can be determined by physiological condition, space, and predation. It may be necessary to account for these sources of mortality when predicting recruitment from larval supply.

Despite these limitations, models of larval transport can help refine existing efforts in intertidal research and conservation. For example, the results of all simulations predicted high larval supply to the Monterey Peninsula between the HMS and SWC sites. Collection of recruitment data in this area could reveal that there is higher larval settlement in southern Monterey Bay that does not reach the monitored sites at HMS and SWC. Alternatively, these data could show that recruitment is similar to the adjacent existing sites, and this information would then be used to adjust the model. In this way, predictions of larval supply can be used to focus sampling programs in the intertidal zone.

Simulation results may be used to examine how populations are connected through larval dispersal. In the

model simulations, successful larvae did not move very far from their release point. In addition to estimating dispersal distances, simulation results show possible paths of larval dispersal. These predictions of larval dispersal are useful for spatially explicit conservation and management efforts. Spatial variability in larval dispersal has a major influence on the effectiveness of marine reserves (e.g., Roberts et al. 2003). These results illustrate the type of information that can be obtained from models of larval dispersal and used for designing marine reserves.

In summary, we have developed a coupled biological–physical model of *B. glandula* dispersal that incorporates larval development as a function of temperature and chlorophyll concentration and migration behavior as a function of larval stage. Dispersal simulations predicted spatial variation in larval supply along the central California coast. In model simulations, relaxation circulation patterns promoted more larval settlement than upwelling circulation patterns, as observed previously by several investigators. More larvae were delivered to the nearshore waters north of Monterey Bay than to the south. For individual intertidal sites around Monterey Bay, larval dispersal patterns differed considerably. Successful larvae dispersed farther on average from the sites to the north of the bay than from sites to the south of the bay. Finally, simulation results suggest that dispersal distances of the majority of successful larvae are limited to tens of kilometers despite the potential for larvae to disperse much farther. Models of larval development and behavior will improve with more observations of the vertical distributions of larvae in the field and the larval behavior that affects these distributions. We also encourage the incorporation of chlorophyll patchiness into physical circulation models. Although uncertainties exist, modeling is one useful tool that may be used to study the dispersal of many intertidal species. This coupled larval dispersal model can easily be adapted to other marine larval species or coastal regions, and similar model simulations can be used to further our understanding of connectivity between intertidal populations.

References

- ALEXANDER, S. E., AND J. ROUGHGARDEN. 1996. Larval transport and population dynamics of intertidal barnacles: A coupled benthic/oceanic model. *Ecol. Monogr.* **66**: 259–275.
- BERTSSON, K. M., P. R. JONSSON, A. I. LARSSON, AND S. HOLDT. 2004. Rejection of unsuitable substrata as a potential driver of aggregated settlement in the barnacle *Balanus improvisus*. *Mar. Ecol. Prog. Ser.* **275**: 199–210.
- BERTNESS, M. D., S. D. GAINES, AND R. A. WAHLE. 1996. Wind-driven settlement patterns in the acorn barnacle *Semibalanus balanoides*. *Mar. Ecol. Prog. Ser.* **137**: 103–110.
- BOTSFORD, L. W. 2001. Physical influences on recruitment to California Current invertebrate populations on multiple scales. *ICES J. Mar. Sci.* **58**: 1081–1091.
- BOUSFIELD, E. L. 1955. Ecological control of the occurrence of barnacles in the Miramichi estuary. *Natl. Mus. Can. Biol. Ser. Bull.* **137**: 1–69.
- BREAKER, L. C., AND W. W. BROENKOW. 1994. The circulation of Monterey Bay and related processes. *Oceanogr. Mar. Biol. Ann. Rev.* **32**: 1–64.

- BROWN, S. K., AND J. ROUGHGARDEN. 1985. Growth, morphology, and laboratory culture of larvae of *Balanus glandula* (Cirripedia: Thoracica). *J. Crust. Biol.* **5**: 574–590.
- CHAI, F., R. C. DUGDALE, T.-H. PENG, F. P. WILKERSON, AND R. T. BARBER. 2002. One dimensional ecosystem model of the equatorial Pacific upwelling system, part I: Model development and silicon and nitrogen cycle. *Deep-Sea Res. II.* **49**: 2713–2745.
- , S. T. LINDLEY, AND R. T. BARBER. 1996. Origin and maintenance of a high NO₃ condition in the equatorial Pacific. *Deep-Sea Res. II.* **43**: 1031–1064.
- CONNOLLY, S. R., B. A. MENGE, AND J. ROUGHGARDEN. 2001. A latitudinal gradient in recruitment of intertidal invertebrates in the northeast Pacific Ocean. *Ecology* **82**: 1799–1813.
- DE WOLF, P. 1973. Ecological observations on the mechanisms of dispersal of barnacle larvae during planktonic life and settling. *Neth. J. Sea Res.* **6**: 1–129.
- FARRELL, T. M., D. BRACHER, AND J. ROUGHGARDEN. 1991. Cross-shelf transport causes recruitment to intertidal populations in central California. *Limnol. Oceanogr.* **36**: 279–288.
- FRANKS, P. J. S. 1992. Sink or swim: Accumulation of biomass at fronts. *Mar. Ecol. Prog. Ser.* **82**: 1–12.
- GAINES, S., S. BROWN, AND J. ROUGHGARDEN. 1985. Spatial variation in larval concentrations as a cause of spatial variation in settlement for the barnacle, *Balanus glandula*. *Oecologia* **67**: 267–272.
- GAINES, S. D., AND J. ROUGHGARDEN. 1987. Fish in offshore kelp forests affect recruitment to intertidal barnacle populations. *Science* **235**: 479–481.
- GRAHAM, W. M., AND J. L. LARGIER. 1997. Upwelling shadows as nearshore retention sites: The example of northern Monterey Bay. *Cont. Shelf Res.* **17**: 509–532.
- GROSBERG, R. K. 1982. Intertidal zonation of barnacles: The influence of planktonic zonation of larvae on vertical distribution of adults. *Ecology* **63**: 894–899.
- HARDY, A. C., AND R. BAINBRIDGE. 1954. Experimental observations on the vertical migrations of plankton animals. *J. Mar. Biol. Assoc. U.K.* **33**: 409–448.
- HAURY, L. R., H. YAMAZAKI, AND E. C. ITSWEIRE. 1990. Effects of turbulent shear flow on zooplankton distribution. *Deep-Sea Res.* **37**: 447–461.
- HODUR, R. M. 1997. The Naval Research Laboratory's coupled ocean/atmosphere mesoscale prediction system (COAMPS). *Mon. Weather Rev.* **125**: 1414–1430.
- JIANG, M.-S., F. CHAI, R. C. DUGDALE, F. WILKERSON, T.-H. PENG, AND R. T. BARBER. 2003. A nitrate and silicate budget in the equatorial Pacific Ocean: A coupled biological–physical model study. *Deep-Sea Res. II* **50**: 2971–2996.
- KNIGHT-JONES, E. W., AND E. MORGAN. 1966. Responses of marine animals to changes in hydrostatic pressure. *Oceanogr. Mar. Biol. Ann. Rev.* **4**: 267–299.
- LANG, W. H., R. B. FORWARD, AND D. C. MILLER. 1979. Behavioral responses of *Balanus improvisus* nauplii to light intensity and spectrum. *Biol. Bull.* **157**: 166–181.
- LUCAS, M. I., G. WALKER, D. L. HOLLAND, AND D. J. CRISP. 1979. An energy budget for the free-swimming and metamorphosing larvae of *Balanus balanoides* (Crustacea: Cirripedia). *Mar. Biol.* **55**: 221–229.
- MCMANUS, M. A., AND OTHERS. 2003. Characteristics, distribution and persistence of thin layers over a 48 hour period. *Mar. Ecol. Prog. Ser.* **261**: 1–19.
- PFEIFFER-HOYT, A. S., AND M. A. MCMANUS. 2005. Modeling the effects of environmental variability on *Balanus glandula* larval development. *J. Plankton Res.* **27**: 1211–1228.
- RAIMONDI, P. T. 1988. Settlement cues and determination of the vertical limit of an intertidal barnacle. *Ecology* **69**: 400–407.
- ROBERTS, C. M., AND OTHERS. 2003. Ecological criteria for evaluating candidate sites for marine reserves. *Ecol. Appl.* **13**: S199–S214.
- ROSENFELD, L. K., F. B. SCHWING, N. GARFIELD, AND D. E. TRACY. 1994. Bifurcated flow from an upwelling center: A cold water source for Monterey Bay. *Cont. Shelf Res.* **14**: 931–964.
- ROUGHGARDEN, J., S. GAINES, AND H. POSSINGHAM. 1988. Recruitment dynamics in complex life cycles. *Science* **241**: 1460–1466.
- , J. T. PENNINGTON, D. STONER, S. ALEXANDER, AND K. MILLER. 1991. Collisions of upwelling fronts with the intertidal zone: The cause of recruitment pulses in barnacle populations of central California. *Acta Oecol.* **12**: 35–51.
- SOTKA, E. E., J. P. WARES, J. A. BARTH, R. K. GROSBERG, AND S. R. PALUMBI. 2004. Strong genetic clines and geographical variation in gene flow in the rocky intertidal barnacle *Balanus glandula*. *Mol. Ecol.* **13**: 2143–2156.
- STRATHMANN, M. F. 1987. Reproduction and development of marine invertebrates of the Northern Pacific coast: Data and methods for the study of eggs, embryos, and larvae. Univ. of Washington.
- STRATHMANN, R. R., E. S. BRANSCOMB, AND K. VEDDER. 1981. Fatal errors in set as a cost of dispersal and the influence of intertidal flora on set of barnacles. *Oecologia* **48**: 13–18.
- WING, S. R., J. L. LARGIER, L. W. BOTSFORD, AND J. F. QUINN. 1995. Settlement and transport of benthic invertebrates in an intermittent upwelling region. *Limnol. Oceanogr.* **40**: 316–329.
- WU, R. S. S., P. K. S. LAM, AND B. S. ZHOU. 1997. Effects of two oil dispersants on phototaxis and swimming behaviour of barnacle larvae. *Hydrobiologia* **352**: 9–16.
- YAMAZAKI, H., AND K. D. SQUIRES. 1996. Comparison of oceanic turbulence and copepod swimming. *Mar. Ecol. Prog. Ser.* **144**: 299–301.

Received: 19 December 2005

Accepted: 18 January 2007

Amended: 2 February 2007